A Low-coordinate Iridium Complex with a Donor-flexible *O,N*-Ligand for Highly Efficient Formic Acid Dehydrogenation

Nicolas Lentz[a] and Martin Albrecht[a*]

[a]Department of Chemistry, Biochemistry and Pharmaceutical Sciences University of Bern Freiestrasse 3, CH-3012 Bern (Switzerland).
*E-mail: martin.albrecht@unibe.ch

ABSTRACT: Formic acid is one of the most promising hydrogen carriers. Here, we report on a highly productive iridium-based catalyst for formic acid dehydrogenation, which is based on an underligated iridium(III) center containing a donor-flexible pyridylidene-amine ligand containing a chelating phenolate. This complex reaches temperature-dependent turnover frequencies from 2,000 (40 °C) to 280,000 h^{-1} (100 °C) and up to 3 million turnover numbers, thus outperforming state-of-the-art systems. The high efficiency together with the remarkably low cost and easy accessibility of the complex (<100 $/g) are attractive features for industrial application.
KEYWORDS: nitrogen ligands, donor flexibility, iridium, formic acid dehydrogenation, hydrogen production,.

Efforts to implement a hydrogen economy as alternative to fossil fuels are critically depending on methods to safely store and controllably release hydrogen.[1–3] A promising approach to reach this goal relies on the use of liquid hydrogen carriers as energy vectors that are undergoing reversible hydrogenation and dehydrogenation cycles. Formic acid (HCOOH, FA) stands out as such a carrier as it is easy to handle, has a sufficiently high hydrogen content (4.4%), and a high energy density (1.77 kWh L^{-1}).[4]

The catalytic hydrogenation of CO_2 to store hydrogen in FA is well established with homogeneous and heterogenous catalyst.[5,6] Concomitantly, hydrogen release through FA dehydrogenation has gained much interest.[7–10] After early work in the late 60s,[11] groundbreaking work by Beller, Dyson and Laurenczy in 2008[12,13] initiated a surge of investigations towards high performance catalysts.[14] Current benchmark systems include the iron complex **I**,[15] which is based on an Earth-abundant iron (Fig. 1a). Iridium complex **II**[14] and ruthenium complex **III** reach higher turnover numbers (TON),[16] while built from precious metals.[17] Further work confirmed the potential of precious metals for high catalytic activity and stability,[18–22] which is attractive for long-term usage subject to proper catalyst recycling. The implementation of such catalytic systems is, however, often hampered by the requirement of sophisticated and expensive ligands to impart high catalytic activity.[23]

Here we demonstrate the benefit of a new class of readily accessible low-cost nitrogen-based ligands to develop dehydrogenation catalysts with outstanding activity and stability. The ligand design is based on a phenoxy-substituted pyridylidene-amine (PYE). PYEs are an underexplored class of ligands[24–26] with unique properties originating from their donor flexibility, represented by either a zwitterionic or a neutral quinoidal limiting resonance structure (**A**, **B** Fig. 1b).[24,25,27] This modularity allows this ligand class to toggle between a π-basic (**A**) and a π-acidic donor site (**B**), with obvious benefits to redox events, as demonstrated by outstanding performance of such systems in oxidation and reduction catalysis.[26,28–30] Here we demonstrate accessibility to an unusual underligated PYE iridium(III) complex and its extraordinary activity and cost efficiency in FA dehydrogenation.

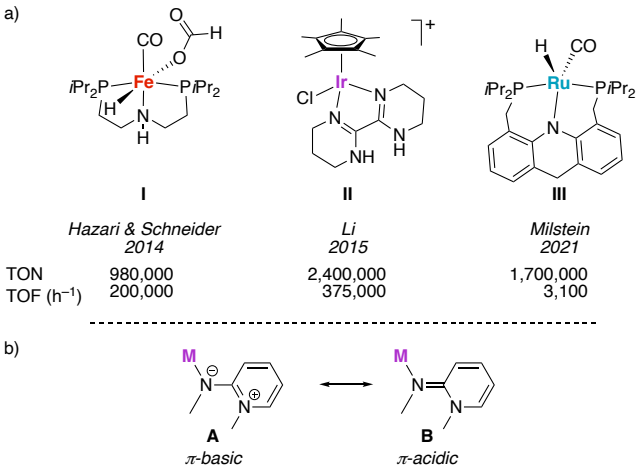

Figure 1. a) State-of-the-art homogeneous formic acid dehydrogenation catalysts **I–III**; b) generic PYE ligand with limiting zwitterionic resonance structure **A** and neutral quinoidal resonance structure **B**.

Ligand precursor **1** was prepared from commercially available and inexpensive 2-aminophenol and 2-chloromethylpyridinium iodide (Scheme 1). Iridium complexation with $[IrCp^*Cl_2]_2$ followed by anion metathesis with $NaPF_6$ afforded complex **2** in excellent 97% yield as an air- and moisture-stable red solid. ^{1}H NMR spectroscopy

showed a diagnostic upfield shift of the N–CH_3 singlet (δ_H = 3.88) and disappearance of the OH and NH singlets at δ_H = 10.21 and 9.99, respectively.

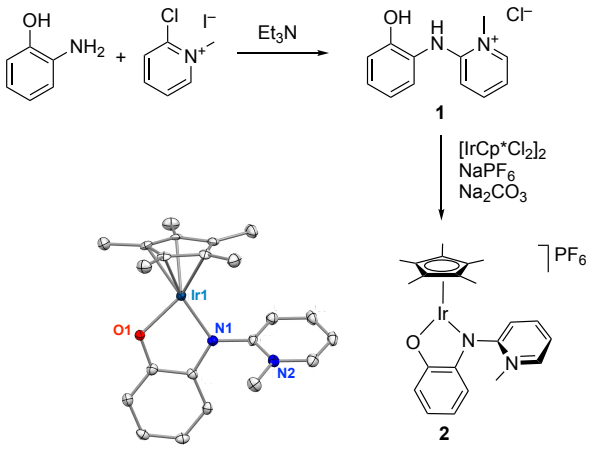

Scheme 1. Synthesis of ligand precursor **1** and iridium complex **2** (ORTEP at 50% probability, H atoms and PF_6^- anion omitted for clarity).

Single crystal X-ray diffraction analysis of complex **2** revealed an iridium complex in an unusual two- rather than three-legged piano-stool geometry in the solid state (Scheme 1, Table S7).[31] The underligated 16e$^-$ configuration is also preserved in solution. Diffusion-ordered NMR spectroscopy (DOSY, Fig. S27) indicated a diffusion parameter of 6.83 x 10^{-10} m^2 s^{-1}, which is commensurate with the theoretical value of the cation in solution (6.77 x 10^{-10} m^2 s^{-1}),[32] and therefore in agreement with a monomeric complex. Moreover, no coordination of donor solvents such as MeCN or DMSO was observed. For example, when complex **2** was dissolved in DMSO and precipitated with toluene, neither coordinated nor free DMSO was observed by ^{1}H NMR measurements in CD_2Cl_2 or acetone-d_6. Albeit underligated, the iridium(III) center of complex **2** is therefore highly stabilized without a further ligand or a formal 18e$^-$ configuration.

Because of the availability of an open coordination site and the flexible donor properties of the PYE-phenolate ligand, complex **2** was evaluated in FA dehydrogenation (Table 1). In the presence of equimolar amounts of FA and sodium formate in DMSO (Table 1 entry 1), H_2 and CO_2 are produced exclusively without any detectable amounts of H_2O or CO (Fig. S12). With 0.1 mol% pre-catalyst loading at 60 °C, FA dehydrogenation reaches 75% within 1 h with a turnover frequency TOF = 2000 h^{-1} (entry 1). The quantity of formate as additive is critical for high catalytic performance, since either an increase or a decrease lowered the catalytic performance (TOF = 1800 and 400 h^{-1} for 2 and 0.5 eq. formate, respectively, and 540 and 250 turnover numbers, TON; entries 2, 3). This observation suggests a delicate role of pH to ensure optimal catalytic activity, in line with related catalysts based on half-sandwich iridium complexes.[18,21,33] The alkali cation of the formate additive has a distinctly promotional effect on the catalytic activity along the series Li > Na > K with TOF values of 2,900, 2,000, and 1,300 h^{-1}, respectively (entries 1, 4 and 5), which may be rationalized by Lewis acid activation of the FA substrate.[15,34] Even at a lower 0.01 mol% catalyst loading, 60% conversion of FA was observed within 1 h with a TOF = 26,000 h^{-1} (entry 6). Variation of the temperature directly impacts the catalytic activity (entries 7–9). At 80 °C, the TOF raises to 82,000 h^{-1}, and at 100 °C even to 280,000 h^{-1}, providing an easy handle to tailor the production and availability of H_2. An Eyring plot of the rates at different temperatures yielded activation parameters $\Delta H^{\ddagger}$ = 74 kJ mol^{-1} and $\Delta S^{\ddagger}$ = –146 J K^{-1} mol^{-1} (Fig. S6). The highly negative entropy factor suggests an associative step such as interaction of an intermediate with a molecule of FA in the turnover-limiting step (*vide infra*).[35]

Table 1. Catalytic FA dehydrogenation with complex **2**.[a]

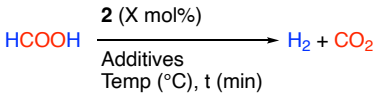

Entry	Additive (mmol)	T (°C)	TON[b]	TOF (h^{-1})[c]
1	HCOONa (1)	60	790	2,000
2	HCOONa (2)	60	650	1,800
3	HCOONa (0.5)	60	440	400
4	HCOOLi (1)	60	810	2,900
5	HCOOK (1)	60	640	1,300
6[d]	HCOOLi (1)	60	6800	26,000
7[d]	HCOOLi (1)	40	2400	2,000
8[d]	HCOOLi (1)	80	8700	82,000
9[d]	HCOOLi (1)	100	9000	280,000

[a] General conditions: complex **2** (1 µmol), HCOOH (1 mmol), additive, and DMSO (1 mL) heated to the indicated temperature; [b] TON measured by a gas flow meter see SI for details; [c] TOF measured at 25% conversion; [d] reduced loading of **2** (0.1 µmol).

In all measurements, a gradual decrease in activity was observed, which was attributed to a change in pH upon consumption of the FA, but not the formate. This interpretation is supported by the change in initial catalytic activity when the relative amount of formate was changed (cf entries 2–4 in Table 1). It is further reinforced by repetitive FA addition experiments, which revealed consistent TOFs around 22,000 h^{-1} when fresh FA batches are added every 30 min (Fig. S9).

To fully explore the robustness of the catalyst under turnover conditions, FA was continuously added using an automatic syringe pump at approximately the same rate as it was consumed, which left the reaction mixture at a constant FA/formate ratio and therefore constant pH. Under these conditions, the catalytic rate was steady for >60 hours at 60 °C (22,000 h^{-1} TOF; Fig. 2). At 100 °C, FA dehydrogenation occurred at a persistent 260,000 h^{-1} for 8 h. After this time and 2.1 M turnovers, catalyst deactivation was observed. For high turnover, the best compromise between high activity and catalyst robustness was 80 °C as reaction temperature. Under these conditions, complex **2** is active for more than 35 h at a steady TOF = 77,000 h^{-1} and reaches 3 million turnovers, thus outperforming the productivity of the most robust catalysts known to date. For example, Milstein's complex **III** requires, in the absence of any additives, 50 days to reach 1.7 M turnovers,[16] while Li's complex **I** accomplishes 2.4 M turnovers in approximatively 14 h.[14] Himeda reported an iridium complex that reaches 10 M, though at very low rate (35 days).[20] In a small scale-up experiment using 0.05 mol% complex **2** and a continuous FA addition (3.7 mL min^{-1}) continuously produced H_2 at >0.6 mL s^{-1}, achieving 57 L gas production and 2,800,000 TONs in 13 h (Fig. S10). We note that under these continuous addition conditions, the quantity of formate additive is negligible relative to FA (1:300 ratio).

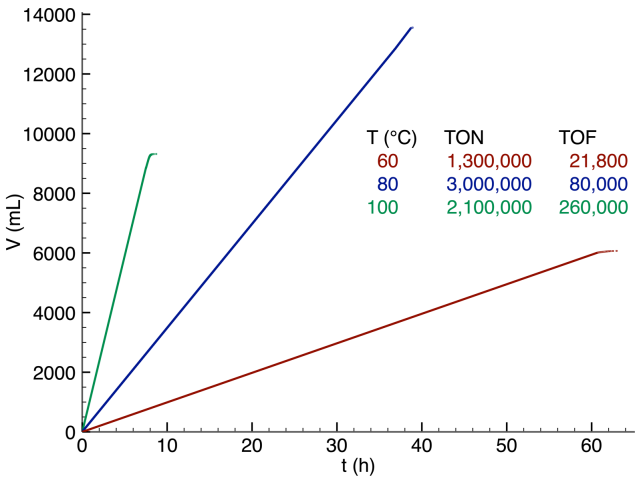

Figure 2. FA dehydrogenation under continuous addition conditions with complex **2** (0.01 mol%) in DMSO (1 mL) starting from a mixture of HCOOH (1 mmol) and HCOOLi (1 mmol) at 100 °C (green; addition at 971 μL h^{-1}), 80 °C (blue; at 292 μL h^{-1}) and 60 °C (red; at 81.5 μL h^{-1}).

The exceptionally high activity of complex **2** combined with the simple synthesis offers potential for industrial application. A cost and productivity analysis indicates that despite the involvement of iridium as precious metal, complex **2** is economically more attractive than other state-of-the-art catalysts, even those based on Earth-abundant iron, since these systems typically use expensive ligands for ensuing catalyst robustness (Table 2; S2–S5). In particular, the low costs for the preparation of the ligand precursor **1** (4.33 $ /g) keep the catalyst price relatively low (96.5 $ /g for **2**, compared to about 290 $ /g for Fe complex **I** and 700 $ /g for Ir complex **II**). Obviously, the costs of **2** are strongly influenced by the market price of iridium, which has been quite volatile due to its low production volume (7,300 kg in 2018) and highly limited Earth-abundance, an effect that may be partially mitigated by the availability of efficient precious metal recycling technologies.[36] The low price of complex **2** together with its exquisite catalytic performance lead to attractively low costs for fuel production. For example, the preparation of 1000 L H_2 is about 5 times cheaper than with the iron **I** (Table 2, S6).

Table 2. Cost and normalized TON and TOF analysis of complex **2** and state-of-the art catalyst for FA dehydrogenation [a]

cat.	T (°C)	cat price ($ /g)	H_2 production costs ($/1000 L)	($h /1000 L)	ref
2	80	96.5	0.90	0.51	this work
2	100	96.5	1.3	0.15	this work
I	80	287	5.3	0.21	14
II	80	700	15.5	0.11	15
III	95	1438	20	14	16

[a] see Tables S2-S5 for price calculation details and Table S6 for H_2 prodcution cost calculations.

Mechanistic insights were obtained from kinetic experiments. Variation of catalyst concentrations (0.10–0.31 mol%) indicate a first order rate-dependence in catalyst (Fig S8). Kinetic isotope experiments using either HCOOH, DCOOH, HCCOD, or DCOOD as substrate were performed with NEt_3 as base rather than formate to avoid any scrambling. The rate markedly decreases with HCOOD compared to HCOOH (KIE = 3.7, Table S1), indicating either rate-limiting O–H bond cleavage or, more likely, protonation of the putative Ir–H intermediate, which is also supported by the strong pH-dependence of the reaction rate (*vide supra*). In contrast, using DCOOH gave only a small KIE = 1.43, suggesting a secondary effect of C–H bond cleavage.

To trap the catalyst resting state, complex **2** was reacted with stoichiometric lithium formate in DMSO–d_6. NMR spectroscopy revealed the instantaneous formation of the iridium hydride complex **3**, rather than any formate complex (Scheme 2). Complex **3** features upfield shifted aromatic signals that indicate a three-legged piano-stool geometry of a neutral iridium(III) species, and a diagnostic hydride resonance at $\delta_H = -11.57$ (Fig. S19). Attempts to isolate and crystallize this hydride species have been precluded by its limited stability ($t_{1/2}$ ~30 min, Fig. S21). Nonetheless, these data are pointing to the formation of a Ir–H intermediate and agree with protonation of this hydride species to form H_2 as the turnover limiting step. This mechanistic scenario is in line with the observed KIEs, the highly negative activation entropy $\Delta S^{\ddagger}$, and the delicate balance on pH. It indicates a behavior distinctly different from most other FA dehydrogenation catalysts, which generally feature the formate adduct as catalyst resting state and ensuing turnover-limiting β-hydrogen elimination.[14,20,33]

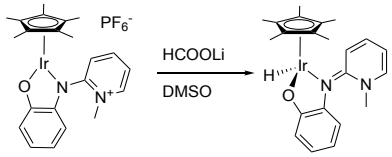

2 3

Scheme 2. Formation of hydride complex **3** from complex **2** and formate.

In summary, we present a simple and remarkably inexpensive iridium complex that is underligated. Key for stabilizing the unusual 16e⁻iridium(III) configuration is the presence of a phenoxy-PYE ligand. The complex is extraordinarily efficient in catalytic FA dehydrogenation and reaches TOFs of almost 300,000 h^{-1} and TONs up to 3,000,000, corresponding to the production of some 100 L hydrogen per mg catalyst. Further optimization of this powerful catalyst is conceivable based on the steric and electronic modularity of both the phenoxy and the PYE ligand units. The mechanistic insights presented here with H_2 formation as turnover-limiting step as well as the pH dependence of the catalytic process will provide valuable guidance for such optimization. Moreover, the N,O-bidentate ligand system may be attractive for a variety of other catalytic systems that benefit from a low-coordinate metal environment.

AUTHOR INFORMATION

Corresponding Author

Martin Albrecht – Department of Chemistry, Biochemistry and Pharmaceutical Sciences, University of Bern, Freiestrasse 3, CH-3012 Bern (Switzerland); orcid.org/0000-0001-7403-2329; E-mail: martin.albrecht@unibe.ch

Author

Nicolas Lentz – Department of Chemistry, Biochemistry and Pharmaceutical Sciences, University of Bern, Freiestrasse 3, CH-3012 Bern (Switzerland); orcid.org/0000-0003-1465-3099

ASSOCIATED CONTENT

Supporting Information: Synthetic and catalytic procedures, gas production profiles, NMR spectra, cost analyses, and crystallographic data (PDF). This information is available free of charge on the ACS Publications website.

Accession Codes: CCDC 2193146 and 2193147 contain the supplementary crystallographic data for this paper. These data can be obtained free of charge via www.ccdc.cam.ac.uk/ data_request/cif, or by emailing data_request@ccdc.cam.ac. uk, or by contacting The Cambridge Crystallographic Data Centre, 12 Union Road, Cambridge CB2 1EZ, UK; fax: +44 1223 336033.

ACKNOWLEDGMENT

We thank the group of Chemical Crystallography of the University of Bern for X-ray analysis and Y. Kong and P. Broekmann for GC analysis and the Swiss National Science Foundation for generous financial support (grant 200020_182663).

.

REFERENCES

(1) van Renssen, S. The Hydrogen Solution? *Nat. Clim. Change* **2020**, *10* (9), 799–801. https://doi.org/10.1038/s41558-020-0891-0.

(2) *The Hydrogen Economy: A Non-Technical Review*; UNEP, Ed.; United Nations Environment Programme: Nairobi, Kenya, 2006, pp1–42.

(3) *Climate Change 2014: Mitigation of Climate Change: Working Group III Contribution to the Fifth Assessment Report of the Intergovernmental Panel on Climate Change*; Intergovernmental Panel on Climate Change, Edenhofer, O., Eds.; Cambridge University Press: New York, NY, 2014, pp1–1435.

(4) Mellmann, D.; Sponholz, P.; Junge, H.; Beller, M. Formic Acid as a Hydrogen Storage Material – Development of Homogeneous Catalysts for Selective Hydrogen Release. *Chem. Soc. Rev.* **2016**, *45* (14), 3954–3988. https://doi.org/10.1039/C5CS00618J.

(5) Weilhard, A.; Argent, S. P.; Sans, V. Efficient Carbon Dioxide Hydrogenation to Formic Acid with Buffering Ionic Liquids. *Nat. Commun.* **2021**, *12* (1), 231. https://doi.org/10.1038/s41467-020-20291-0.

(6) Wei, D.; Sang, R.; Sponholz, P.; Junge, H.; Beller, M. Reversible Hydrogenation of Carbon Dioxide to Formic Acid Using a Mn-Pincer Complex in the Presence of Lysine. *Nat. Energy* **2022**, *7* (5), 438–447. https://doi.org/10.1038/s41560-022-01019-4.

(7) Kumar, A.; Daw, P.; Milstein, D. Homogeneous Catalysis for Sustainable Energy: Hydrogen and Methanol Economies, Fuels from Biomass, and Related Topics. *Chem. Rev.* **2022**, *122* (1), 385–441. https://doi.org/10.1021/acs.chemrev.1c00412.

(8) Guo, J.; Yin, C. K.; Zhong, D. L.; Wang, Y. L.; Qi, T.; Liu, G. H.; Shen, L. T.; Zhou, Q. S.; Peng, Z. H.; Yao, H.; Li, X. B. Formic Acid as a Potential On-Board Hydrogen Storage Method: Development of Homogeneous Noble Metal Catalysts for Dehydrogenation Reactions. *ChemSusChem* **2021**, *14* (13), 2655–2681. https://doi.org/10.1002/cssc.202100602.

(9) Onishi, N.; Himeda, Y. Recent Advances in Homogeneous Catalysts for Hydrogen Production from Formic Acid and Methanol. In *CO2 Hydrogenation Catalysis*; Himeda, Y., Ed.; Wiley, 2021; pp 259–283. https://doi.org/10.1002/9783527824113.ch10.

(10) Sordakis, K.; Tang, C.; Vogt, L. K.; Junge, H.; Dyson, P. J.; Beller, M.; Laurenczy, G. Homogeneous Catalysis for Sustainable Hydrogen Storage in Formic Acid and Alcohols. *Chem. Rev.* **2018**, *118* (2), 372–433. https://doi.org/10.1021/acs.chemrev.7b00182.

(11) Coffey, R. S. The Decomposition of Formic Acid Catalysed by Soluble Metal Complexes. *Chem. Commun. Lond.* **1967**, No. 18, 923b. https://doi.org/10.1039/c1967000923b.

(12) Loges, B.; Boddien, A.; Junge, H.; Beller, M. Controlled Generation of Hydrogen from Formic Acid Amine Adducts at Room Temperature and Application in H_2/O_2 Fuel Cells. *Angew. Chem. Int. Ed.* **2008**, *47* (21), 3962–3965. https://doi.org/10.1002/anie.200705972.

(13) Fellay, C.; Dyson, P.; Laurenczy, G. A Viable Hydrogen-Storage System Based On Selective Formic Acid Decomposition with a Ruthenium Catalyst. *Angew. Chem. Int. Ed.* **2008**, *47* (21), 3966–3968. https://doi.org/10.1002/anie.200800320.

(14) Wang, Z.; Lu, S.-M.; Li, J.; Wang, J.; Li, C. Unprecedentedly High Formic Acid Dehydrogenation Activity on an Iridium Complex with an *N*,*N*′-Diimine Ligand in Water. *Chem. - Eur. J.* **2015**, *21* (36), 12592–12595. https://doi.org/10.1002/chem.201502086.

(15) Bielinski, E. A.; Lagaditis, P. O.; Zhang, Y.; Mercado, B. Q.; Würtele, C.; Bernskoetter, W. H.; Hazari, N.; Schneider, S. Lewis Acid-Assisted Formic Acid Dehydrogenation Using a Pincer-Supported Iron Catalyst. *J. Am. Chem. Soc.* **2014**, *136* (29), 10234–10237. https://doi.org/10.1021/ja505241x.

(16) Kar, S.; Rauch, M.; Leitus, G.; Ben-David, Y.; Milstein, D. Highly Efficient Additive-Free Dehydrogenation of Neat Formic Acid. *Nat. Catal.* **2021**, *4* (3), 193–201. https://doi.org/10.1038/s41929-021-00575-4.

(17) Boddien, A.; Mellmann, D.; Gärtner, F.; Jackstell, R.; Junge, H.; Dyson, P. J.; Laurenczy, G.; Ludwig, R.; Beller, M. Efficient Dehydrogenation of Formic Acid Using an Iron Catalyst. *Science* **2011**, *333* (6050), 1733–1736. https://doi.org/10.1126/science.1206613.

(18) Kanega, R.; Onishi, N.; Wang, L.; Murata, K.; Muckerman, J. T.; Fujita, E.; Himeda, Y. Picolinamide-Based Iridium Catalysts for Dehydrogenation of Formic Acid in Water: Effect of Amide N Substituent on Activity and Stability. *Chem. – Eur. J.* **2018**, *24* (69), 18389–18392. https://doi.org/10.1002/chem.201800428.

(19) Lu, S.-M.; Wang, Z.; Wang, J.; Li, J.; Li, C. Hydrogen Generation from Formic Acid Decomposition on a Highly Efficient Iridium Catalyst Bearing a Diaminoglyoxime Ligand. *Green Chem.* **2018**, *20* (8), 1835–1840. https://doi.org/10.1039/C8GC00495A.

(20) Onishi, N.; Kanega, R.; Fujita, E.; Himeda, Y. Carbon Dioxide Hydrogenation and Formic Acid Dehydrogenation Catalyzed by Iridium Complexes Bearing Pyridyl-Pyrazole Ligands: Effect of an Electron-Donating Substituent on the Pyrazole Ring on the Catalytic Activity and Durability. *Adv. Synth. Catal.* **2019**, *361* (2), 289–296. https://doi.org/10.1002/adsc.201801323.

(21) Kanega, R.; Ertem, M. Z.; Onishi, N.; Szalda, D. J.; Fujita, E.; Himeda, Y. CO_2 Hydrogenation and Formic Acid Dehydrogenation Using Ir Catalysts with Amide-Based Ligands. *Organometallics* **2020**, *39* (9), 1519–1531. https://doi.org/10.1021/acs.organomet.9b00809.

(22) Guzmán, J.; Urriolabeitia, A.; Polo, V.; Fernández-Buenestado, M.; Iglesias, M.; Fernández-Alvarez, F. J. Dehydrogenation of Formic Acid Using Iridium-NSi Species as Catalyst Precursors. *Dalton Trans.* **2022**, *51* (11), 4386–4393. https://doi.org/10.1039/D1DT04335H.

(23) Dutta, I.; Chatterjee, S.; Cheng, H.; Parsapur, R. K.; Liu, Z.; Li,

Z.; Ye, E.; Kawanami, H.; Low, J. S. C.; Lai, Z.; Loh, X. J.; Huang, K. Formic Acid to Power towards Low-Carbon Economy. *Adv. Energy Mater.* **2022**, *12* (15), 2103799. https://doi.org/10.1002/aenm.202103799.

(24) Slattery, J.; Thatcher, R. J.; Shi, Q.; Douthwaite, R. E. Comparison of Donor Properties of N-Heterocyclic Carbenes and N-Donors Containing the 1H-Pyridin-(2E)-Ylidene Motif. *Pure Appl. Chem.* **2010**, *82* (8), 1663–1671. https://doi.org/10.1351/PAC-CON-09-11-10.

(25) Leigh, V.; Carleton, D. J.; Olguin, J.; Mueller-Bunz, H.; Wright, L. J.; Albrecht, M. Solvent-Dependent Switch of Ligand Donor Ability and Catalytic Activity of Ruthenium(II) Complexes Containing Pyridinylidene Amide (PYA) N-Heterocyclic Carbene Hybrid Ligands. *Inorg. Chem.* **2014**, *53* (15), 8054–8060. https://doi.org/10.1021/ic501026k.

(26) Doster, M. E.; Johnson, S. A. Selective C-F Bond Activation of Tetrafluorobenzenes by Nickel(0) with a Nitrogen Donor Analogous to N-Heterocyclic Carbenes. *Angew. Chem. Int. Ed.* **2009**, *48* (12), 2185–2187. https://doi.org/10.1002/anie.200806048.

(27) Shi, Q.; Thatcher, R. J.; Slattery, J.; Sauari, P. S.; Whitwood, A. C.; McGowan, P. C.; Douthwaite, R. E. Synthesis, Coordination Chemistry and Bonding of Strong N-Donor Ligands Incorporating the 1 *H* -Pyridin-(2 *E*)-Ylidene (PYE) Motif. *Chem. - Eur. J.* **2009**, *15* (42), 11346–11360. https://doi.org/10.1002/chem.200901382.

(28) Melle, P.; Thiede, J.; Hey, D. A.; Albrecht, M. Highly Efficient Transfer Hydrogenation Catalysis with Tailored Pyridylidene Amide Pincer Ruthenium Complexes. *Chem. – Eur. J.* **2020**, *26* (58), 13226–13234. https://doi.org/10.1002/chem.202001145.

(29) Salzmann, K.; Segarra, C.; Albrecht, M. Donor-Flexible Bis(Pyridylidene Amide) Ligands for Highly Efficient Ruthenium-Catalyzed Olefin Oxidation. *Angew. Chem. Int. Ed.* **2020**, *59* (23), 8932–8936. https://doi.org/10.1002/anie.202002014.

(30) Bertini, S.; Henryon, D.; Edmunds, A. J. F.; Albrecht, M. Pyridylidene Amide Ru Complex for Selective Oxidation in Organic Synthesis. *Org. Lett.* **2022**, *24* (6), 1378–1382. https://doi.org/10.1021/acs.orglett.2c00177.

(31) Ringenberg, M. R.; Nilges, M. J.; Rauchfuss, T. B.; Wilson, S. R. Oxidation of Dihydrogen by Iridium Complexes of Redox-Active Ligands. *Organometallics* **2010**, *29* (8), 1956–1965. https://doi.org/10.1021/om9010593.

(32) Evans, R.; Deng, Z.; Rogerson, A. K.; McLachlan, A. S.; Richards, J. J.; Nilsson, M.; Morris, G. A. Quantitative Interpretation of Diffusion-Ordered NMR Spectra: Can We Rationalize Small Molecule Diffusion Coefficients? *Angew. Chem.* **2013**, *125* (11), 3281–3284. https://doi.org/10.1002/ange.201207403.

(33) Kawanami, H.; Iguchi, M.; Himeda, Y. Ligand Design for Catalytic Dehydrogenation of Formic Acid to Produce High-Pressure Hydrogen Gas under Base-Free Conditions. *Inorg. Chem.* **2020**, *59* (7), 4191–4199. https://doi.org/10.1021/acs.inorgchem.9b01624.

(34) Heimann, J. E.; Bernskoetter, W. H.; Hazari, N. Understanding the Individual and Combined Effects of Solvent and Lewis Acid on CO_2 Insertion into a Metal Hydride. *J. Am. Chem. Soc.* **2019**, *141* (26), 10520–10529. https://doi.org/10.1021/jacs.9b05192.

(35) Upadhyay, S. Temperature Effect on Reaction Rate. In *Chemical Kinetics and Reaction Dynamics*; Springer Netherlands: Dordrecht, 2006; pp 46–54. https://doi.org/10.1007/978-1-4020-4547-9_2.

(36) Eggert, R. G. Minerals Go Critical. *Nat. Chem.* **2011**, *3* (9), 688–691. https://doi.org/10.1038/nchem.1116.

For Table of Contents Entry Only